

# Prediction of nominal wake of a semi-displacement high-speed vessel at full scale

Ugur Can<sup>\*1</sup> and Sakir Bal<sup>2</sup>

<sup>1</sup>Department of Naval Architecture and Marine Engineering, Yildiz Technical University, Istanbul, Turkey

<sup>2</sup>Department of Naval Architecture and Marine Engineering, Istanbul Technical University, Istanbul, Turkey

(Received October 20, 2021, Revised January 28, 2022, Accepted March 15, 2022)

**Abstract.** In this study, the nominal wake field of a semi-displacement type high-speed vessel was computed at full scale by using CFD (Computational Fluid Dynamics) and GEOSIM-based approaches. A scale effect investigation on nominal wake field of benchmark Athena vessel was performed with two models which have different model lengths. The members of the model family have the same Fr number but different Re numbers. The spatial components of nominal wake field have been analyzed by considering the axial, radial and tangential velocities for models at different scales. A linear feature has been found for radial and tangential components while a nonlinear change has been obtained for axial velocity. Taylor wake fraction formulation was also computed by using the axial wake velocities and an extrapolation technique was carried out to get the nonlinear fit of nominal wake fraction. This provides not only to observe the change of nominal wake fraction versus scale ratios but also to estimate accurately the wake fraction at full-scale. Extrapolated full-scale nominal wake fractions by GEOSIM-based approach were compared with the full-scale CFD result, and a very good agreement was achieved. It can be noted that the GEOSIM-based extrapolation method can be applied for estimation of the nominal wake fraction of semi-displacement type high-speed vessels.

**Keywords:** full-scale athena hull; GEOSIM series; nominal wake fraction; scale effect

## 1. Introduction

Nominal wake region of high-speed vessels differs from that of conventional displacement type of ships. A particular consideration is needed to calculate the nominal wake fraction because the wake characteristics have a very crucial role on a successful design of the propulsion system. Scale effect is another important issue that should be considered in the hydrodynamic design stage and the examination of it shows some differences from classical displacement type of vessels because of significant change of flow field at high speeds.

It is known that there are generally two components of nominal wake field, the viscous wake and the pressure wake. The viscous wake component (friction) usually dominates the wake flow for displacement type of vessels. On the other hand the pressure wake is significant for high-speed vessels especially for planing types (Odabasi and Fitzsimmons 1978). Semi-displacement type of high-speed vessels have hybrid hydrodynamic characteristics with a round bilge form. Therefore, it is hard to make a straightforward assessment for wake surveys of semi-displacement high-speed

---

\*Corresponding author, Ph.D. Student, E-mail: ugurcan@yildiz.edu.tr

vessels.

In the past, Savitsky and Morabito (2010) was conducted comprehensive experimental studies with stepped planing hulls to analyze and develop empirical formulations for longitudinal nearfield wake profiles. Beigi and Manshadi (2020) have carried out a computational study about the effect of the measurement location on wake field of submarines and they found that the near location to the considered geometry produces non-uniform velocity profiles. Gray-Stephens *et al.* (2020a) have made an experimental study on longitudinal nearfield wake and compared their results with those of empirical approach and linear wake assumption. They mentioned more successful estimation of empirical formulation given by Savitsky and Morabito than linear wake assumption. Gray-Stephens *et al.* (2020b) have also performed a computational investigation on the nominal wake field of a planing hull by using a transient RANS (Reynolds Averaged Navier Stokes) solver and the results at various velocities and trim angles have been presented. Authors mentioned that CFD results are the most accurate ones over empirical or linear approaches.

There are also some other experimental and numerical studies on wake field of semi-displacement type of high-speed vessels. The experimental studies were conducted for benchmark Athena hull at David Taylor Naval Ship Research and Development Center. Effective wake survey for fully appended model scale results were given by Hurwitz and Crook (1980) and comparison of sea trials was made for wake field at model scale by Day Jr *et al.* (1980). Bhushan *et al.* (2009) have investigated how the wake field is affected by different turbulence modelling properties for fully appended Athena hull both at model scale and full-scale. They compared the computational results with EFD (Experimental Fluid Dynamics) results given by Jenkins (1984) and their wake field results with a rough wall function had a better agreement with those of experiments.

In this study, a GEOSIM (GEOMETRICALLY SIMILAR) family has been generated with two different model scales of Athena hull. First a GEOSIM-series was used as suggested by Telfer (1927). It is a known approach to investigate the resistance, effective wake or propulsive parameters in computational studies (Can *et al.* 2020, Delen *et al.* 2020, Dogrul *et al.* 2020). The nominal wake fraction results have also been extrapolated for displacement type KCS ship in the study of Delen and Bal (2019). Can and Bal (2022) have computed principal hydrodynamic forces of Athena hull and conducted a full-scale extrapolation by GEOSIM based extrapolation strategy. Here a modified version of the GEOSIM-based extrapolation method was performed for estimation of nominal wake fraction of a semi-displacement type high-speed vessel. Extrapolated results with the modified GEOSIM method have been compared with those of CFD at full-scale and the accuracy of extrapolation approach was checked out. Change of wake field with different scale ratios, including full-scale for each spatial component such as axial, radial and tangential velocities was also discussed in this study. These computational results have been presented in detail.

## 2. Mathematical and numerical modelling

### 2.1 Governing equations

Three dimensional, fully turbulent flow is modeled as incompressible and time dependent during the computational study. The governing equations are given here. First the continuity equation for incompressible flow is as follows

$$\frac{\partial U_i}{\partial x_i} = 0 \quad (1)$$

and the RANS equation can be expressed in short form below:

$$\frac{\partial U_i}{\partial t} + \frac{\partial(U_i U_j)}{\partial x_j} = -\frac{1}{\rho} \frac{\partial P}{\partial x_i} + \frac{\partial(-\overline{u'_i u'_j})}{\partial x_j} + \nu \frac{\partial^2 U_i}{\partial x_j^2} \quad (2)$$

$i$  and  $j$  subscripts show directions of the cartesian coordinate system and  $U$ ,  $P$ ,  $\rho$ ,  $\nu$  are the mean velocity, mean pressure, fluid density and kinematic viscosity, respectively.  $(\overline{u'_i u'_j})$  term is the Reynolds stress term, and this term was handled by the realizable  $k$ - $\varepsilon$  turbulence model which is a modified version of the standard two-equational model.

In the standard version of the  $k$ - $\varepsilon$  model, two additional transport equation is used to solve principal turbulence parameters which are turbulence kinetic energy ( $k$ ) and rate of dissipation ( $\varepsilon$ ) as follows

$$\frac{\partial k}{\partial t} + \frac{\partial}{\partial x_j} (k \cdot U_j) = \tau_{ij} \frac{\partial U_i}{\partial x_j} - \varepsilon - \frac{\partial}{\partial x_j} \left[ \left( \nu + \frac{\nu_t}{\sigma_k} \right) \frac{\partial k}{\partial x_j} \right] \quad (3)$$

$$\frac{\partial \varepsilon}{\partial t} + \frac{\partial}{\partial x_j} (\varepsilon U_j) = C_{s1} \frac{\varepsilon}{k} \tau_{ij} \frac{\partial U_i}{\partial x_j} - C_{s2} \frac{\varepsilon^2}{k} + \frac{\partial}{\partial x_j} \left[ \left( \nu + \frac{\nu_t}{\sigma_\varepsilon} \right) \frac{\partial \varepsilon}{\partial x_j} \right] \quad (4)$$

Here  $\nu_t$  is the turbulence viscosity and it is calculated by  $(\nu_t = C_\mu \frac{k^2}{\varepsilon})$ . Other parameters are statistical turbulence coefficients and  $(C_{\varepsilon 1}=1.44, C_{\varepsilon 2}=1.92, C_\mu=0.09, \sigma_k=1.0, \sigma_\varepsilon=1.3)$ , respectively. Further information can be obtained from (Wilcox 1993).

## 2.2 Ship geometry and main particulars

Athena has a round bilge form and transom stern with a skeg. Model 5365 is a common literature scale of Athena hull ( $\lambda=8.25$ ). It was used in computational and experimental studies (Jenkins, 1984; Ratcliffe *et al.* 2008, Duman *et al.* 2018). In this computational study, two different scaled models were used to generate GEOSIM series with a scale ratio of ( $\lambda=8.25$ ) given in literature and an additional scale ratio ( $\lambda=5.5$ ). Main particulars of the GEOSIM model family and full-scale Athena hull are presented in Table 1. Here M1, M2, FS represent the model 1, model 2 and full-scale, respectively. The 3D geometry of the Athena hull is given in Fig. 1.

## 2.3 Modified Telfer's GEOSIM method

The scale effect is an important issue that should be investigated properly. Understanding the change of wake fraction between model and full scales is possible by reducing the scale ratio for the geometrically similar forms at a constant Fr number. The concept of GEOSIM series was proposed by Telfer to understand the effects of scaling and to include it in the calculation process of design (Telfer 1927).

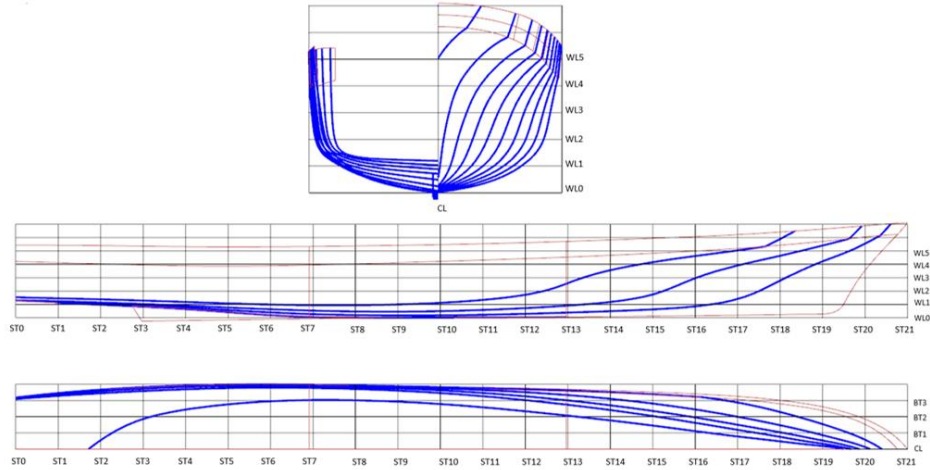


Fig. 1 Athena R/V line plans (top: front view, station lines, middle: profile view, buttock lines: bottom: top view, waterlines)

Table 1 Main particulars of the model family and full-scale of Athena hull

Parameter (Unit)	M1	M2	FS
Scale ratio, $\lambda$	8.25	5.5	1.0
Length between perpendicular, $L_{PP}$ (m)	5.685	8.527	46.9
Breadth, B (m)	0.836	1.255	6.9
Draft, $T_H$ (m)	0.180	0.272	1.498
Static wetted surface area, $S_0$ (m <sup>2</sup> )	4.222	9.500	287.360
Displacement, $\Delta$ (kg)	375.91	1268.69	211078.92
Velocity, V (m/s)	5.974	7.317	17.160
Froude, Fr		0.80	

The method was originally applied to ship resistance problem by generating a model family and establishing a relationship between model scales and full-scale. Total ship resistance ( $C_D$  as nondimensional coefficient) is represented by establishing a relationship between model and full-scale results without any decomposition process as follows (Bertram 2012)

$$C_D = f(\log Re^{-1/3}) \quad (5)$$

This equation can be modified for nominal wake fraction ( $w_N$ ) in terms of logarithmic Re number. The equation is given below for nominal wake fraction

$$w_N = \frac{a}{(\log Re)^x} \quad (6)$$

The normalized form nominal wake fraction ( $w'_N$ ) is also given as

$$w'_N = \frac{w_N}{\log Re} = \frac{a'}{(\log Re)^{x'}} \quad (7)$$

The regression coefficients in Eqs. (6) and (7)  $a$ ,  $a'$  and  $x$ ,  $x'$  are calculated by using two different scale ratios and a nonlinear curve fitting method. Taylor wake formula can be used to compute the nominal wake fractions as follows

$$w_N = \frac{V_S - V_A}{V_S} \quad (8)$$

here  $V_S$  is the ship velocity and  $V_A$  is the mean velocity at the propeller disk.

#### 2.4 Numerical modelling

The FVM method has been used to discretize the governing equations by using commercial Star CCM+ software. A segregated flow strategy was adapted to the solution and the coupling between pressure and velocity variables was ensured by SIMPLE (Semi-Implicit Method for Pressure-Linked Equations) method. Second order upwind scheme for convective terms and first order Euler implicit scheme for transient terms in the governing equation were used to construct the numerical solution.

The multiphase flow field has been modeled by VOF (Volume of Fluid) method (Hirt and Nichols 1981). Time step was specified by considering the formula suggested by ITTC for computational studies in ship hydrodynamics:  $[0.005 \sim 0.01L/V]$ . Here,  $L$  is the length and  $V$  is the velocity (ITTC 2011).

In this computational study, flow field is fully turbulent due to high  $Re$  number at each scale ratio and the turbulence was modeled by executing the realizable  $k$ - $\epsilon$  turbulence model which is a two-equational turbulence model and a suitable option for ship hydrodynamics studies (ITTC 2011). The  $k$ - $\epsilon$  model also gives advantages in computational cost almost %25 according to the  $k$ - $\omega$  model (Quérard *et al.* 2008). Furthermore, realizable model can handle some problems of the standard model such as over prediction of turbulence viscosity in some flow fields which include a big flow separation or high-level mean shear rate. An additional damping term was added to provide dissipation in turbulence viscosity and correct the physical modelling. Two possible scenarios can be applied during near wall modelling. First, near wall region is modeled without using any wall function and this condition is ensured by keeping  $y^+$  under 1 ( $y^+ < 1$ ). Second and more common option is using wall function and moving  $y^+$  to relatively larger values ( $30 < y^+ < 300$ ). In this study, second option was preferred and two-layer  $y^+$  treatment was performed for near wall modelling. This wall function enables both low- and high-level  $y^+$  values to satisfy the general  $y^+$  condition in the range between 30-300 for most parts of the geometry and to avoid some local regions which have lower  $y^+$  values ( $y^+ < 1$ ) such as stagnation points around the geometry.

The computational domain should have appropriate dimensions to catch physical features of the flow field and limit the element numbers and computational cost. ITTC recommendations have been considered while dimensions of the computational domain were selected (ITTC 2011). The dimensions are  $(-3.6 \leq x/L_{PP} \leq 2.8, 0 \leq y/L_{PP} \leq 2.4, -2.1 \leq z/L_{PP} \leq 1.6)$  of upstream ( $x$ ), transverse ( $y$ ) and vertical direction ( $z$ ), respectively. At the entry region to the computational domain, uniform

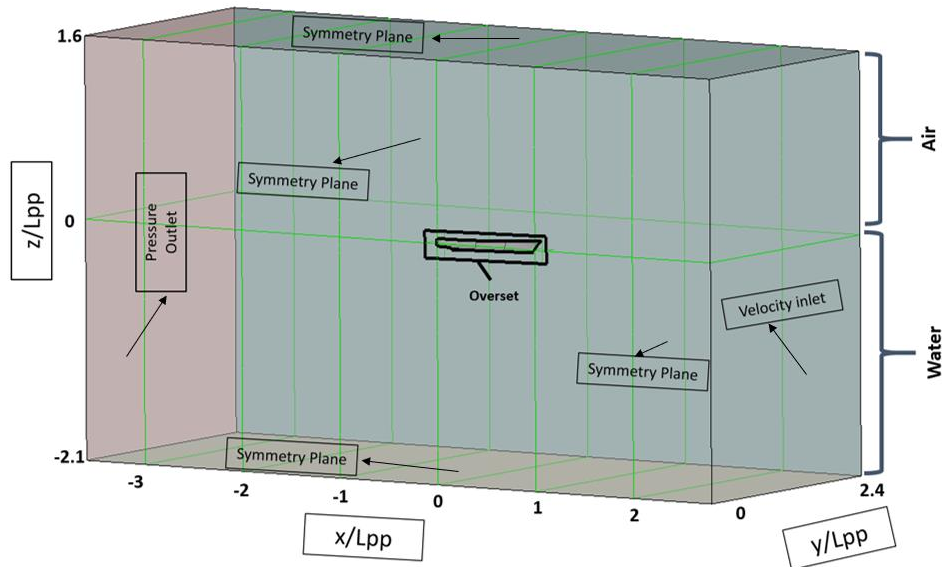


Fig. 2 Numerical towing tank for 2DOF Athena and applied boundary conditions

velocity distribution was defined as velocity inlet boundary condition. Zero pressure gradient condition was assigned as pressure outlet to the exit side of the domain. Hull surfaces were defined as no-slip walls and normal and tangential velocities were equal to zero. Other boundaries which are hull midplane section, far side of the domain in transversal direction, bottom and top regions were defined as symmetry boundaries. Normal velocities were zero since tangential velocities were nonzero values along these boundary faces. General view of the domain, main dimensions and type of the boundaries are shown in Fig. 2.

Spatial discretization was made by using trimmer mesh algorithm. The algorithm uses cartesian cut-cell method to generate hexahedral dominant mesh structure in the computational domain. Local mesh refinements can be achieved by creating sub-volumetric controls and a finer mesh can be generated there. These refinements are needed where the high flow gradients occur, and this kind of refinement strategy was adapted in this study. Mesh structure of bow, stern and overall geometry for hull and free surface region for whole computational domain was refined and finer mesh regions were obtained in these regions. Hull geometry was defined as free to heave and pitch motions by using DFBI (Dynamic Fluid Body Interaction) method. Mesh deformation arising from the vertical motion was acquired by overset mesh technique which is an efficient way of modelling mesh deformation over time (Stern *et al.* 2013). The method is highly appropriate especially for high-speed marine vehicles because of relatively higher vertical motion response than displacement type of vessels (Sukas *et al.* 2017). General view of the mesh structure of M1 model scale is given in Fig. 3. Local refinement regions were placed where the high flow gradients occur such as, bow and stern regions. Free surface plane and the overset region as a box which surrounded the hull geometry were also considered as high gradient regions so local refinements were performed in those regions. These refined mesh regions can also be seen in Fig. 3. Mesh structures of the other model scale (M2) and full-scale was systemically refined in terms of scale ratio.

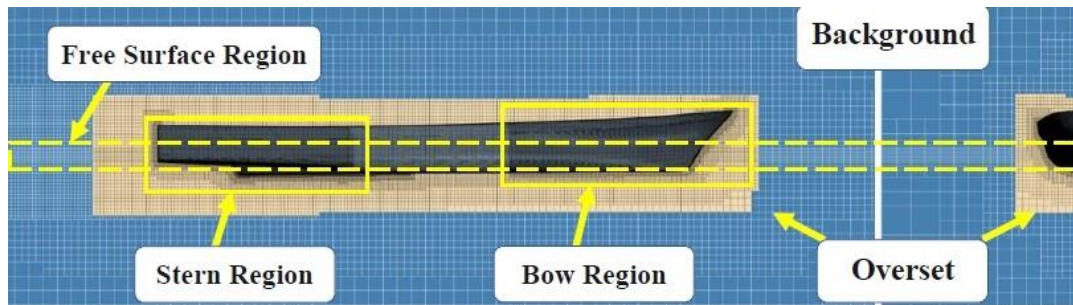


Fig. 3 Mesh structure around the hull geometry for M1 model of Athena hull (left: profile, right: front view)

### 3. Numerical results

A nominal wake survey has been performed for Athena hull with a skeg which is a semi-displacement type high-speed vessel. A GEOSIM family was generated by considering a common literature scale (M1:  $\lambda=8.25$ ) and an additional model scale (M2:  $\lambda=5.5$ ). Full-scale hull geometry has also been included to the computational study for comparison. First, a verification study was conducted to ensure the established numerical setup in this study, and spatial discretization was only examined because it is the predominant component of overall uncertainty. M1 model scale was used for verification study and the outputs was implemented systematically to the spatial discretization of other members of the model family in terms of the scale ratio. After that, nominal wake fields are given in detail by presenting each spatial component separately. The components are given together for GEOSIM series to figure out the scaling effect clearly on nominal wake fraction. Behavior of the axial and the other components (radial and tangential) of velocity with scale ratios has been discussed. Wake fraction was computed by using the axial component of nominal wake and the GEOSIM extrapolation approach based on modified Telfer's method. Therefore, the scaling became a part of the nominal wake estimation at full-scale by putting it in the extrapolation equation versus Re number.

#### 3.1 Verification and validation study

GCI (Grid Convergence Index) method was used to estimate the numerical uncertainty. The method was first proposed by Roache (1998) and various modifications were then implemented to improve the method. Today, GCI method is a very common and suitable method for computational ship hydrodynamics (ITTC 2011). The spatial discretization is usually dominant in computational studies, therefore only the uncertainty arisen from spatial discretization was considered. The uncertainty procedure suggested by Celik *et al.* (2008) has been used for verification and the method is explained briefly in this section.

Total resistance coefficient of M1 model of Athena hull was analyzed for uncertainty estimation. The computations were made for half of the geometry because of symmetrical form of Athena hull. With the uncertainty computation, the specified mesh structure was kept fixed and adapted to the other scales.

N1, N2, N3 are three different mesh sets which have different refinement ratios and  $\phi_1$ ,  $\phi_2$  and  $\phi_3$  are the associated result parameters correspond to each mesh structure in verification analyses. Refinement ratios are as follows

$$r_{21} = \frac{h_2}{h_1}, r_{32} = \frac{h_3}{h_2} \quad (9)$$

Selection of the refinement rates are important for quality of the verification analyses and Celik *et al.* (2008) mentioned that the values should be kept above 1.3 ( $r > 1.3$ ). Some other computational studies applied a higher refinement rate as  $\sqrt{2}$  (Ozdemir *et al.* 2016, Kumar and Vijayakumar 2020).

$\varepsilon_{21}$  and  $\varepsilon_{32}$  are the differences between the results of successive grid structures such as ( $\varepsilon_{21} = \phi_2 - \phi_1$  and  $\varepsilon_{32} = \phi_3 - \phi_2$ ) and the convergence condition ( $R$ ) is computed as

$$R = \frac{\varepsilon_{21}}{\varepsilon_{32}} \quad (10)$$

There are three scenarios as a result of verification studies. First, mesh set can be monotonically convergent with the satisfied condition ( $0 < R < 1$ ). Second, it can be oscillatory convergent with the condition ( $-1 < R < 0$ ), otherwise the result is divergence of the mesh set. The results of uncertainty study with the verification parameters are presented in Table 2. Notice that  $R$  parameter satisfies the monotonically convergence condition ( $R=0.52$ ). Furthermore, the uncertainty was obtained in a satisfactory level which is almost ( $GCI = 0.53\%$ ). As a result of the uncertainty analyses, N1 grid has been selected for the computational study.

Computational and experimental results are presented in Table 3 for comparison. Here  $C_D$  and  $\% \Delta C_D$  are given in Eqs. (11) and (12), respectively. This validation study has been performed for total resistance and trim values of M1 model. Relative differences are computed as 3.82% and 2.85% for resistance and trim, respectively. These relative differences are in a satisfactory level for validation study.

$$\% \Delta C_D = 100 \times \left( \frac{C_D (CFD) - C_D (EFD)}{C_D (EFD)} \right) \quad (11)$$

and drag forces are nondimensionalized by the following formula

$$C_D = \frac{F_D}{0.5 \rho S_0 V^2} \quad (12)$$

Table 2 Verification results of the uncertainty analyses for bare Athena hull at  $Fr=0.8$

Parameter	M1 Model
$N1$	$1.630 \times 10^6$
$N2$	$0.984 \times 10^6$
$N3$	$0.670 \times 10^6$
$\phi_1 \times 10^3$	$4.077 \times 10^{-3}$
$\phi_2 \times 10^3$	$4.098 \times 10^{-3}$
$\phi_3 \times 10^3$	$4.141 \times 10^{-3}$
$R$	0.52
$GCI_{fine}^{21}$	0.53%

Table 3 CFD and EFD (Jenkins, 1984) results of total drag and trim values for M1 scale of Athena hull at  $Fr=0.8$

	$C_D \times 10^3$	$\tau$	$\% \Delta C_D$	$\% \Delta \tau$
CFD	4.543	0.994	3.82%	2.85%
EFD	4.376	0.967	-	-

### 3.2 Results for nominal wake

Nominal wake fractions of model family and full-scale Athena hull with a skeg are presented here. Experimental wake field characteristics of Athena hull have been provided by several studies for various conditions such as different velocities and measurement locations around propeller, with and without propeller cases or model/full-scale results (Day Jr *et al.* 1980, Hurwitz and Crook 1980). In this study, the computational results present a higher velocity than those of given in the literature with ( $Fr=0.8$ ) while the maximum Fr in these studies is ( $Fr=0.6$ ).

First, nondimensional wake velocities are shown at a shifted propeller plane in the forward direction. General view of the measurement plane is given in Fig. 4. Note that the Athena model has twin propellers and shaft angle ( $\beta= 8.5^\circ$ ). The measurement plane was translated because the hull geometry has no appendages, and a high shaft angle takes the propeller disk away from the geometry. For these reasons, the wake field is measured at that plane ( $0.052L_{PP}$  in +x direction) and  $0.75R$  radial location was preferred to present results. The geometric representation of the propeller plane is given in Fig. 5 with the radial location and nominal wake components as axial ( $U_z$ ), radial ( $U_R$ ) and tangential ( $U_\theta$ ). Wake velocities of each component are given in Figs. 6-8 for axial, radial and tangential ones, respectively. Here  $z$ ,  $r$  and  $\theta$  subscripts are used to represent axial, radial and tangential components of the wake velocities, respectively. Notice that the axial velocities increase regularly from smaller scale ratios to the full-scale while other components are almost same in a nondimensional form. The axial component is dependent to the scale effect clearly, while the other components have not affected with the change of model length in the nondimensional form. This means that the axial wake velocity has a nonlinear relation with the scale ratio while the other wake components (radial and tangential) have almost linear change.

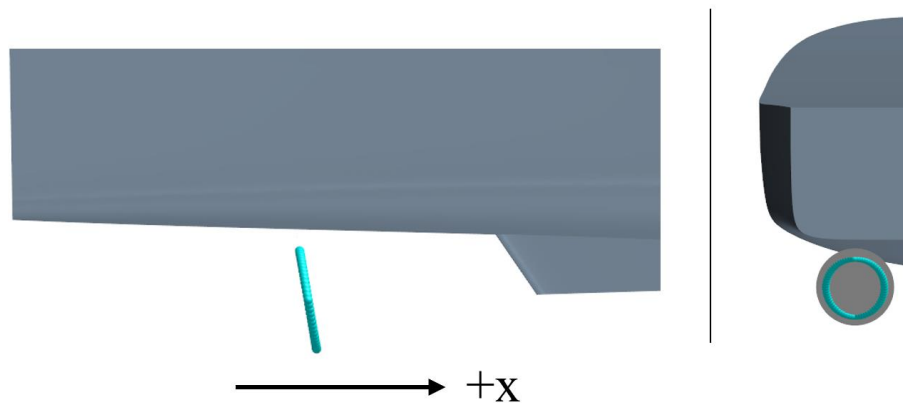


Fig. 4 Measurement Plane:  $0.052L_{PP}$  in +x from propeller disk and  $0.75R$  in radial location (left: profile, right: back view)

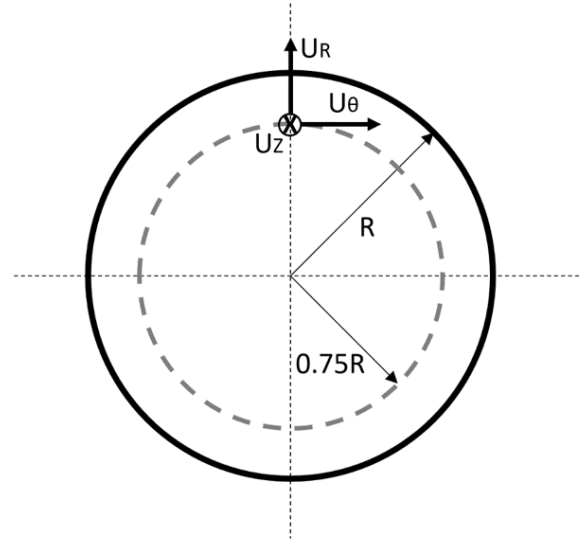


Fig. 5 Representation of the measured nominal wake components on  $0.75R$  radial location of the propeller plane: Axial ( $U_z$ ), radial ( $U_R$ ) and tangential ( $U_\theta$ )

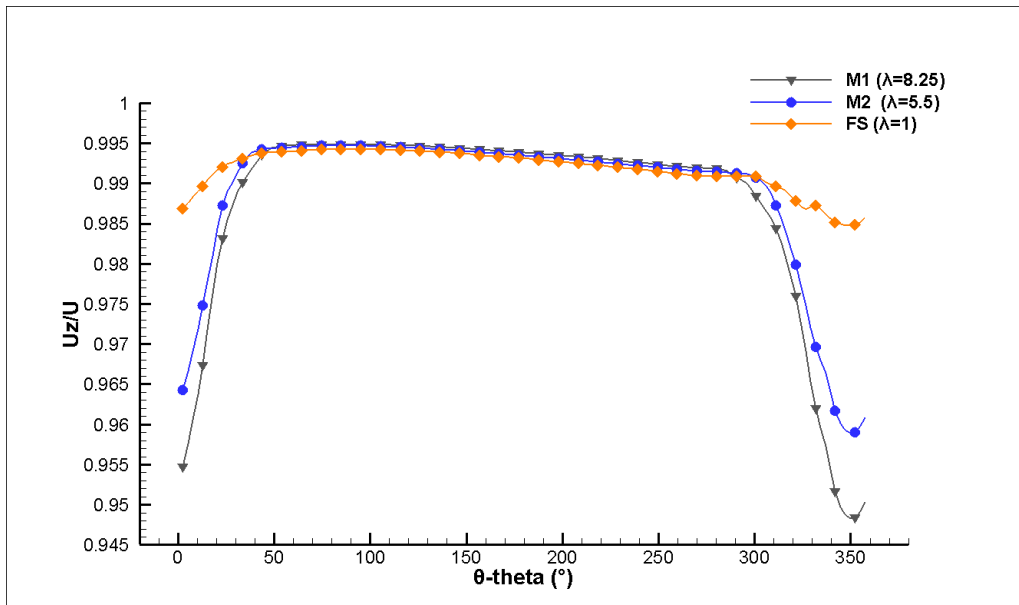


Fig. 6 Nondimensional axial velocities at the measurement plane for all scales of Athena hull at  $Fr=0.8$

The GEOSIM extrapolation was used to predict the full-scale nominal wake fraction by using model-scaled results and obtaining a Re number-based regression equation according to Eqs. (6) and (7). Re number is an indicator of the scale effect for the geometrically similar models at a constant Fr number, therefore establishing a Re number-based regression function has provide an extrapolation approach which completely includes the hydrodynamic effects of scaling and

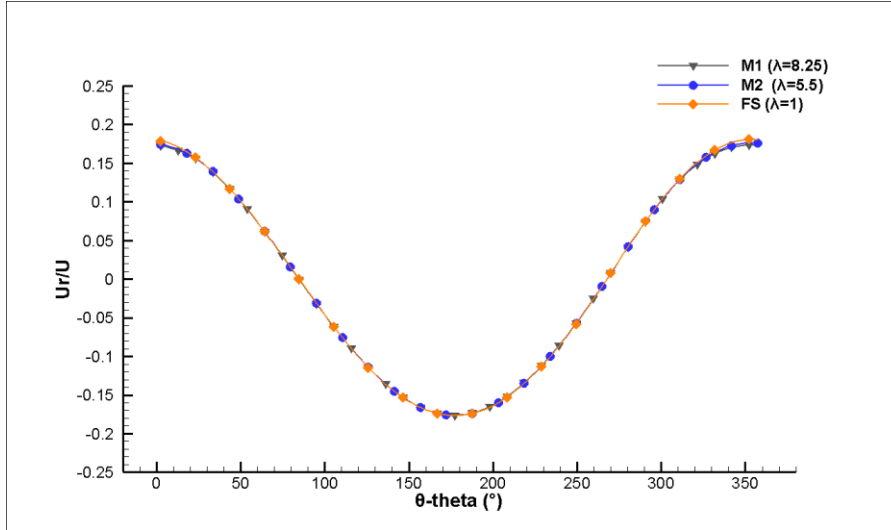


Fig. 7 Nondimensional radial velocities at the measurement plane for all scales of Athena hull at  $Fr=0.8$

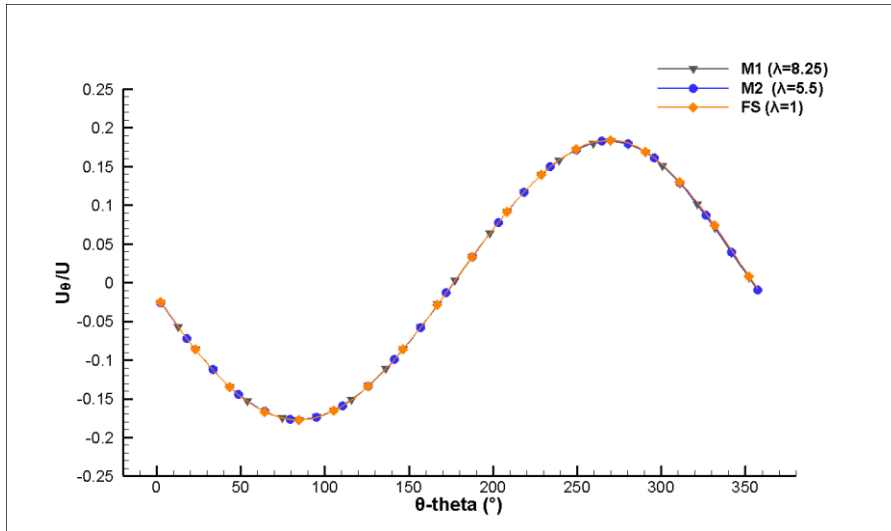


Fig. 8 Nondimensional tangential velocities at the measurement plane for all scales of Athena hull at  $Fr=0.8$

combining viscous and pressure-based effects together in the computation process. The GEOSIM method was executed by using two wake fractions at different scale ratios and putting those in Eq. (6) directly or in Eq. (7) by the normalization process. After that, a nonlinear curve fitting method was applied the data set and regression coefficients were obtained. Therefore, the "nominal wake fraction curve" was plotted for Athena hull at  $Fr=0.8$  with the obtained regression coefficients and general equations in Eqs. (6) and (7). This curve represents the trend of the nominal wake fraction of Athena hull with the increasing Re number from the model scales to the full-scale. The nominal wake fraction curve and extrapolated result by the GEOSIM method are presented in Fig. 9 with the CFD results including full-scale one.

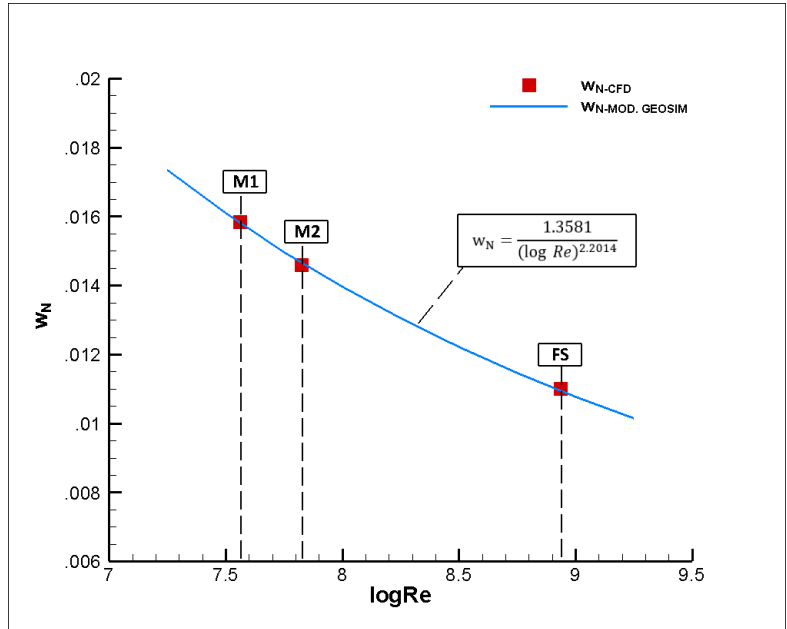


Fig. 9 Comparison of nominal wake fraction results by CFD and GEOSIM extrapolation methods (red symbols: CFD results, blue solid line: GEOSIM extrapolation curve)

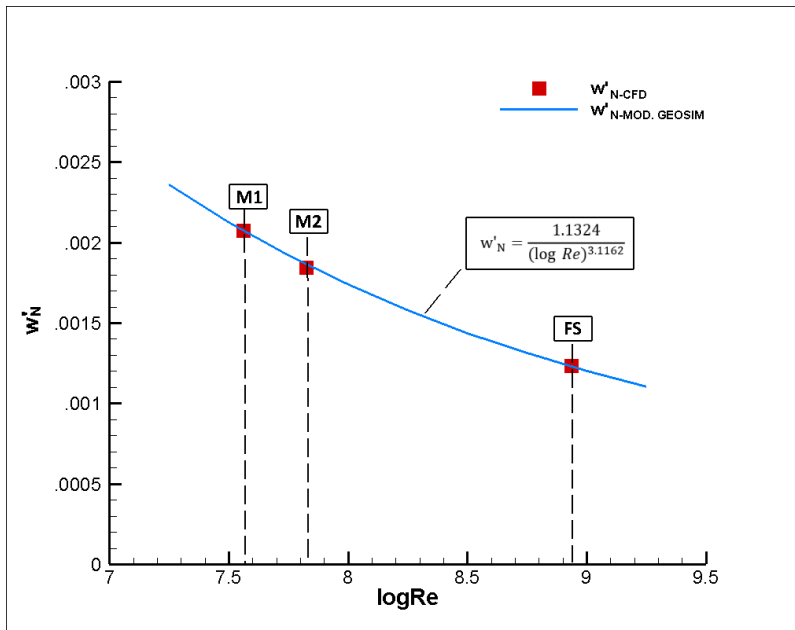


Fig. 10 Comparison of normalized nominal wake fraction results by CFD and GEOSIM extrapolation methods (red symbols: CFD results, blue solid line: GEOSIM extrapolation curve)

In Fig. 10, the nominal wake fractions are normalized with Re number as  $(w'_N = w_N / \log Re)$  and these normalized model-scaled wake fractions are used in Eq. (7). With this normalization process, a more successful estimation has been expected at full-scale and its effects on the

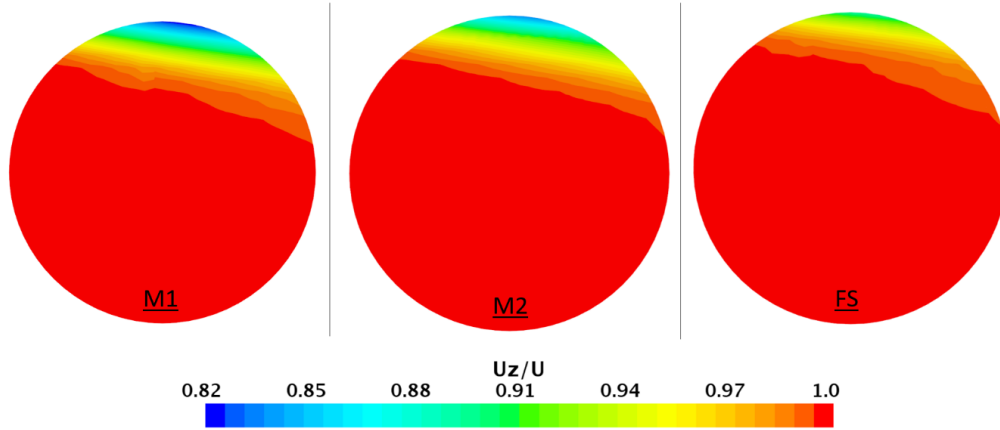


Fig. 11 Nondimensional axial velocities at the measurement plane for all scales of Athena hull at  $Fr=0.8$

Table 4 Comparison of the nominal wake fractions at full-scale by CFD and modified GEOSIM extrapolation methods

	CFD	Mod. GEOSIM
$w_N \times 10^2$	1.099	1.093
$\% \Delta w_N$	-	0.49%
$w_N' \times 10^3$	1.230	1.230
$\% \Delta w_N'$	-	0.12%

extrapolated result are examined by considering the relative differences at full-scale with and without Re number normalization.

Nondimensional axial velocity distribution on the port side propeller disk is also given in Fig. 11 for all scale ratios. Notice that the asymmetrical distribution is appeared in contour plots because of the twin propeller system. Increase of the nominal velocities is also clear from model scale to the full-scale.

The full-scale nominal wake fractions by modified GEOSIM based method with the full-scale CFD result are given in Table 4. Relative differences were calculated as follows:

$$\% \Delta w_N = 100 \times \left( \frac{w_{N(GEOSIM)} - w_{N(CFD)}}{w_{N(CFD)}} \right) \quad (13)$$

There is a very good agreement between both results.

#### 4. Conclusions

In this study, the nominal wake field of a benchmark semi-displacement type high-speed vessel, Athena R/V hull, were analyzed computationally by using a GEOSIM-based approach. Scale effects on the nominal wake field of the Athena hull were examined with two different scaled models and the full-scale CFD results. Beside Fr similarity, Re number has been included to the extrapolation

approach and an accurate extrapolation for nominal wake characteristics was obtained. Two important outcomes from this study can be stated about the wake fields of semi-displacement type high-speed vessels.

- Axial component of wake velocities highly depends on scale effect and increases in a nonlinear manner as the model length increases.
- Radial and tangential wake components are almost independent of scale effect in a nondimensional form and can be extrapolated linearly from model to the full-scale.

Nominal wake fractions (only axial velocities) were used during the extrapolation process because of the linear behavior of the other components (radial and tangential ones). These wake fractions were placed at the nonlinear regression equation and “nominal wake fraction curve” has been obtained by modified GEOSIM method. Extrapolation to the full-scale was easily made by using the nominal wake fraction curve. Consequently, extrapolated results at full-scale are compared with the full-scale CFD result. Modified GEOSIM result is in a very good agreement with the full-scale CFD ( $\% \Delta w_N = 0.49\%$ ). Moreover, the normalization process of nominal wake fractions with the associated Reynolds number at each scale ratio was improved the accuracy of the modified GEOSIM method ( $\% \Delta w_N' = 0.12\%$ ) and the relative difference has decreased according to full-scale CFD result.

## References

- Beigi, S.M., Shateri, A. and Manshadi, M.D. (2020), “Numerical investigation of the effect of the location of stern planes on submarine wake flow”, *Ocean Syst. Eng.*, **10**(3), 289-316. <https://doi.org/10.12989/ose.2020.10.3.289>.
- Bertram, V. (2012), “Resistance and Propulsion”, *Practical Ship Hydrodynamics*, 73-141. <https://doi.org/10.1016/b978-0-08-097150-6.10003-x>.
- Bhushan, S. *et al.* (2009), “Model-and full-scale URANS simulations of athena resistance, powering, seakeeping, and 5415 maneuvering”, *J. Ship Res.*, **53**(4), 179-198. <https://doi.org/10.5957/jsr.2009.53.4.179>.
- Can, U. and Bal, S. (2022), “Prediction of drag and lift forces of a high-speed vessel at full scale by CFD-based GEOSIM method”, *Proceedings of the Institution of Mechanical Engineers Part M: Journal of Engineering for the Maritime Environment*. <https://doi.org/10.1177/14750902211070743>.
- Can, U., Delen, C. and Bal, S. (2020), “Effective wake estimation of KCS hull at full-scale by GEOSIM method based on CFD”, *Ocean Eng.*, 218. <https://doi.org/10.1016/j.oceaneng.2020.108052>.
- Celik, I.B. *et al.* (2008), “Procedure for estimation and reporting of uncertainty due to discretization in CFD applications”, *J. Fluid. Eng. T. ASME*, **130**(7), 0780011–0780014. <https://doi.org/10.1115/1.2960953>.
- Day Jr, W.G., Reed, A.M. and Hurwitz, R.B. (1980), *Full-Scale Propeller Disk Wake Survey and Boundary Layer Velocity Profile Measurements on the 154-Foot Ship R/V Athena*. DAVID W TAYLOR NAVAL SHIP RESEARCH AND DEVELOPMENT CENTER BETHESDA MD SHIP ....
- Delen, C. and Bal, S. (2019), “Telfer’s GEOSIM method revisited by CFD”, *Int. J. Maritime Eng.*, **161**(4), 467-478. <https://doi.org/10.3940/rina.ijme.2019.a4.563>.
- Delen, C., Can, U. and Bal, S. (2020) “Prediction of resistance and self-propulsion characteristics of a full-scale naval ship by CFD-based GEOSIM method”, *J. Ship Res.*, 1-16. <https://doi.org/10.5957/josr.03200022>.
- Dogrul, A., Song, S. and Demirel, Y.K. (2020), “Scale effect on ship resistance components and form factor”, *Ocean Eng.*, **209**, 107428. <https://doi.org/10.1016/j.oceaneng.2020.107428>.
- Duman, S., Sener, B. and Bal, S. (2018), “LCG effects on resistance, lift and trim characteristics of R/V Athena hull”, *Int. J. Small Craft Technol.*, **160**, 43-56.
- Gray-Stephens, A., Tezdogan, T. and Day, S. (2020a), “Experimental measurement of the nearfield longitudinal wake profiles of a high-speed prismatic planing hull”, *Ship Technol. Res.*, **68**(2), 102-128.

- <https://doi.org/10.1080/09377255.2020.1836552>.
- Gray-Stephens, A., Tezdogan, T. and Day, S. (2020b), “Numerical modelling of the nearfield longitudinal wake profiles of a high-speed prismatic planing hull”, *J. Mar. Sci. Eng.*, **8**(7), 516. <https://doi.org/10.3390/jmse8070516>.
- Hirt, C.W. and Nichols, B.D. (1981), “Volume of fluid (VOF) method for the dynamics of free boundaries”, *J. Comput. Phys.*, **39**(1), 201-225. [https://doi.org/10.1016/0021-9991\(81\)90145-5](https://doi.org/10.1016/0021-9991(81)90145-5).
- Hurwitz, R.B. and Crook, L.B. (1980), *Analysis of Wake Survey Experimental Data for Model 5365 Representing the R/V ATHENA in the DTNSRDC Towing Tank*. DAVID W TAYLOR NAVAL SHIP RESEARCH AND DEVELOPMENT CENTER BETHESDA MD SHIP ....
- ITTC (2011), “Practical Guidelines for Ship CFD Applications”, *ITTC – Recommended Procedures and Guidelines ITTC*, 1-8.
- Jenkins, D.S. (1984), *Resistance Characteristics of the High Speed Transom Stern Ship R/V Athena in the Bare Hull Condition*. Report, David W. Taylor Naval Ship Research and Development Center Bethesda Md, USA.
- Kumar, Y.H. and Vijayakumar, R. (2020), “Effect of flap angle on transom stern flow of a High speed displacement Surface combatant”, *Ocean Syst. Eng.*, **10**(1), 1-23. <https://doi.org/10.12989/ose.2020.10.1.001>.
- Ozdemir, Y.H. *et al.* (2016), “A numerical application to predict the resistance and wave pattern of Krisko container ship”, *Brodogradnja*, **67**(2), 47-65. <https://doi.org/10.21278/brd67204>.
- Quéraud, A., Temarel, P. and Turnock, S.R. (2008), “Omae2008-57 330”, *Proceedings of the ASME 27th International Conference on Offshore Mechanics and Arctic Engineering*.
- Ratcliffe, T. *et al.* (2008), “An Integrated Experimental and Computational Investigation into the Dynamic Loads and Free-surface Wave-Field Perturbations Induced by Head-Sea Regular Waves on a 1/8.25 Scale-Model of the R/V ATHENA”, (October), 5-10. Available at: <http://arxiv.org/abs/1410.1935>.
- Roache, P.J. (1998), “Verification of codes and calculations”, *AIAA J.*, **36**(5).
- Savitsky, D. and Morabito, M. (2010), “Surface wave contours associated with the forebody wake of stepped planing hulls”, *Marine Technology and SNAME News*, **47**(1), 1-16. <https://doi.org/10.5957/mtsn.2010.47.1.1>.
- Stern, F. *et al.* (2013), “Computational ship hydrodynamics: Nowadays and way forward”, *Int. Shipbuild. Progress*, **60**(1-4), 3-105. <https://doi.org/10.3233/ISP-130090>.
- Sukas, O.F. *et al.* (2017), “Hydrodynamic assessment of planing hulls using overset grids”, *Appl. Ocean Res.*, **65**, 35-46. <https://doi.org/10.1016/j.apor.2017.03.015>.
- Telfer, E.V. (1927), “Ship resistance similarity”, *T. Roy. Inst. Naval Archit.*, **93**, 174-190.
- Wilcox, D.C. (1993), *Turbulence modeling for CFD*. La Canada, Calif.: DCW Industries.
- Yucel Odabasi, A. and Fitzsimmons, P.A. (1978), “Alternative methods for wake quality assessment”, *Int. Shipbuild. Progress*, **25**(282), 34-42. <https://doi.org/10.3233/isp-1978-2528202>.